Supporting Information

THERMODYNAMIC, ENERGY EFFICIENCY, AND POWER DENSITY ANALYSIS OF REVERSE ELECTRODIALYSIS POWER GENERATION WITH NATURAL SALINITY GRADIENTS

NGAI YIN YIP,[†] DAVID A. VERMAAS,[‡§] KITTY NIJMEIJER,[§] AND MENACHEM ELIMELECH[†*]

[†] Department of Chemical and Environmental Engineering
Yale University
New Haven, CT 06520-8286, USA

[‡] Wetsus, Centre of Excellence for Sustainable Water Technology
P.O. Box 1113, 8900 CC, Leeuwarden, The Netherlands

[§] Membrane Science & Technology
University of Twente, MESA+ Institute for Nanotechnology
P.O. Box 217, 7500 AE, Enschede, The Netherlands

(* E-mail: menachem.elimelech@yale.edu)

REVERSE ELECTRODIALYSIS MODEL

Potential Across a Reverse Electrodialysis Cell. One RED cell, comprising a high concentration (HC) solution compartment separated from two low concentration (LC) solution half-compartments by a pair of cation exchange membrane (CEM) and anion exchange membrane (AEM), is shown in Figure 1B of the main manuscript and reproduced below. Due to the ion concentration difference, the Nernst potential across each ion exchange membrane (IEM), $\xi_{½\text{emf}}$, of the reverse electrodialysis (RED) cell is[1]

$$\xi_{\frac{1}{2}\text{emf}} = \frac{\alpha R_g T}{zF} \ln \frac{\gamma_{HC} x_{HC}}{\gamma_{LC} x_{LC}} \tag{S1}$$

where α is the permselectivity of the IEM, R_g is the gas constant, T is the absolute temperature, z is the ion valence (e.g., z = 1 for Na^+ and Cl^-), and F is the Faraday constant. The activity coefficient and the mole fraction of the ion are denoted by γ and x, respectively, while subscripts HC and LC indicate the high and low concentration solutions, respectively. Permselectivity, α, describes the ability of the membrane to allow the preferential migration of counter ions over co-ions. An α of 1 signifies a perfectly selective ion exchange membrane that permits only counter ion flux and completely excludes co-ions.

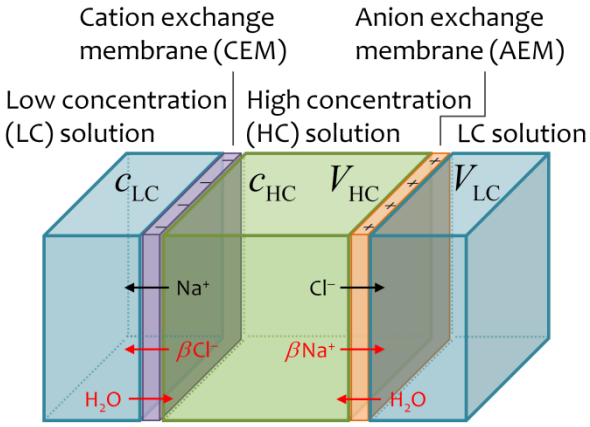

Figure 1B. Schematic of a reverse electrodialysis process. One RED cell is presented, comprising a high concentration (HC) solution compartment (salt concentration c_{HC} and volume V_{HC}) separated from two low concentration (LC) solution half-compartments (salt concentration c_{LC} and combined volume V_{LC}) by a cation exchange membrane (CEM) possessing fixed negative charges and an anion exchange membrane (AEM) having fixed positive charges. Cations and anions permeate across the CEM and AEM, respectively, from the HC solution to the LC solution.

Our previous study found that the effect of γ on the ln(γx) term is relatively small (~5.4-9.3% difference) for the salt concentrations considered here.[2] To simplify the analyses, solution ideality can be assumed (i.e., γ = 1) without significantly affecting accuracy. Further, the volumetric contribution of salt is negligible compared to water for ideal solutions. Thus, $x \approx \nu_{+/-} c \bar{V}$, where $\nu_{+/-}$ is the number of cations or anions each salt molecule dissociates into (e.g., $\nu_+ = \nu_- = 1$ for NaCl), c is the molar salt concentration, and $\bar{V}$ is the molar volume of pure water. The potential (or electromotive force, emf) of the one-cell RED, ξ_{emf}, incorporating the above approximations, is obtained by summing the potential across the CEM and AEM:

$$\xi_{\text{emf}} = \xi_{\frac{1}{2}\text{emf,CEM}} + \xi_{\frac{1}{2}\text{emf,AEM}} \approx \left(\frac{\alpha_{\text{CEM}}}{z_+} + \frac{\alpha_{\text{AEM}}}{z_-} \right) \frac{R_g T}{F} \ln \frac{c_{\text{HC}}}{c_{\text{LC}}} \tag{1}$$

where the subscript of α denotes cation or anion exchange membrane, and the subscript of z represents the cation (+) or anion (–), respectively. Note that $\nu_{+/-}$ and $\bar{V}$ cancel out in the concentration ratio.

Mole Fraction Approximation to Volumetric Fraction. The relative mixing proportions between the low and high concentration solutions is described by ϕ: the ratio of the initial total moles of both water and salt in the LC solution, n_{LC}^0, to the total moles in the system, $n_{\text{LC}}^0 + n_{\text{HC}}^0$. For the relatively dilute solutions considered in this study, the volumetric and mole contribution of salt to the solution is negligible compared to water. Thus, the solution volume and the total number of moles in solution are approximately the volume of water and the moles of water, respectively, and ϕ is approximately the volumetric ratio of the initial LC solution to the total system volume: $\phi \equiv n_{\text{LC}}^0 / \left(n_{\text{LC}}^0 + n_{\text{HC}}^0 \right) \approx V_{\text{LC}}^0 / \left(V_{\text{LC}}^0 + V_{\text{HC}}^0 \right)$.

REVERSE ELECTRODIALYSIS POWER GENERATION CIRCUIT

Internal Resistance of One RED Cell. In an actual RED salinity battery, the stack components are not ideally conductive but possess resistance that impedes the ionic and electric current. The stack resistance, r_{stack}, is the sum of the stack elements in series,[3-5] as depicted in the RED schematic shown in Figure 1A of the main manuscript:

$$r_{\text{stack}} = \frac{N}{A}\left(\text{ASR}_{\text{CEM}} + \text{ASR}_{\text{AEM}} + \frac{d_{\text{HC}}}{\kappa_{\text{HC}}} + \frac{d_{\text{LC}}}{\kappa_{\text{LC}}} \right) + r_{\text{el}} \quad \text{(S2)}$$

where N is the number of membrane pairs (or repeating RED cells), A is the effective cell area, d is the intermembrane distance, κ is the solution electrical conductivity, and r_{el} is the resistance of the end electrodes and redox couple compartment. The resistive property of the IEMs is described by the area specific resistance, ASR; dividing ASR by A yields the membrane resistance (i.e., larger membrane areas contribute less resistance to the stack). The four terms in the parentheses denote the contribution to resistance from CEM, AEM, HC solution compartment, and LC solution compartment, respectively, as indicated by the subscripts, while the term after the brackets represents the electrode resistance. The resistance of the elements is assumed to be ohmic and membrane resistance is taken to be independent of the surrounding salt concentration.[5, 6]

For the one repeating RED cell considered in Figure 1B of the main manuscript, the area specific resistance, ASR_{cell}, is the product of r_{stack} (eq S2) and A, divided by the number of membranes pairs, N:

$$\text{ASR}_{\text{cell}} = r_{\text{cell}}A = \frac{r_{\text{stack}}A}{N} \approx \text{ASR}_{\text{AEM}} + \text{ASR}_{\text{CEM}} + \frac{1}{\Lambda}\left(\frac{d_{\text{HC}}}{c_{\text{HC}}} + \frac{d_{\text{LC}}}{c_{\text{LC}}} \right) \quad (7)$$

where Λ is the molar conductivity of NaCl solution and c is the solution molar concentration. The product of molar conductivity and concentration yields the solution conductivity ($\kappa = \Lambda c$). For the NaCl salt concentrations considered in this study, Λ is calculated to be 0.08798 $\text{mScm}^{-1}\text{mM}^{-1}$ from the linear regression of κ against c (R^2 = 0.996 for $0<c<1$ M NaCl).[7] For RED salinity batteries with a large number of repeating membrane pairs, the contribution of r_{el} to one RED cell is relatively small due to normalization by N and, thus, can be neglected.[4]

During RED, ions permeate across the ion exchange membranes and c_{HC} declines while the LC solution salt concentration rises. As such, the area specific resistance changes as RED progresses. Figure S3 shows representative plots of ASR_{cell} as a function of the fraction of salt permeated, $\Delta n_{\text{s}} / \Delta n_{\text{s}}^{f}$, for $\phi = 0.5$. The HC solution is seawater, while LC solution is river water or brackish water (Figures S3A and S3B, respectively). The ASR of the CEMs and AEMs is taken to be 3.0 Ωcm^2 (typical values of commercial and laboratory-fabricated membranes

reported in literature ranges between ~0.7-11 Ωcm^2),[8, 9] while the distance between the AEM and CEM, d, is 150 μm (intermembrane distance of ~60-500 μm has been investigated in previous RED studies).[4, 5, 10, 11] The total ASR of the one-cell RED (solid black lines) and the contribution from each stack element: CEM and AEM (dash-dotted red lines), LC solution chamber (dotted blue lines), and HC solution chamber (dashed green lines) are presented on logarithmic scales in Figure S3.

At first, when $\Delta n_s = 0$, ASR_{cell} is highest at 120 Ωcm^2 for the seawater-river water system (Figure S3A). The large resistance of the RED cell is mostly attributed to the very low initial salt concentration of the river water LC solution (c_{LC}^0 = 1.5 mM or 88 mg/L NaCl) that gives rise to nearly all the impedance ($d_{LC}/\Lambda c_{LC}$ = 114 Ωcm^2). As ions are transported into the LC solution, ASR_{LC} decreases inversely to c_{LC} and the resulting area specific resistance of the RED cell declines precipitously. The resistance of the IEMs remains constant during RED and dominates ASR_{cell} for the remainder of the process. For example in the representative plot shown in Figure S3A, ASR_{CEM} + ASR_{AEM} accounts for 51% and 66% of ASR_{cell} when $\Delta n_s / \Delta n_s^f$ is 0.1 and 0.2, respectively, and the eventual ASR_{cell} is 7.1 Ωcm^2 while the total membrane resistance is 6.0 Ωcm^2. A similar trend is observed when brackish water (17 mM or 1 g/L NaCl) LC solution is paired with seawater HC solution (Figure S3B), but with a lower initial ASR_{cell} (16.3 Ωcm^2) because of the higher initial brackish water salt concentration compared to river water.

RED POWER GENERATION WITH IMPERFECT SELECTIVITY ION EXCHANGE MEMBRANES

Ion Exchange Membrane Selectivity Imperfections. Ion exchange membranes (IEMs) are thin-films of water-swollen polymers that possess a high concentration of fixed negative (for CEMs) or positive charges (for AEMs) that allows the selective permeation of counter-ions by Donnan exclusion.[8, 12, 13] Actual IEMs do not exclude co-ions perfectly and some co-ions leak across the membranes during RED. Additionally, water diffuses from the low concentration (LC) to the high concentration (HC) solution (i.e., osmosis) and water molecules also are dragged across the membranes by the migration of charged ions (termed "electro-osmosis").[14-16] These phenomena, along with the equations describing them, are presented here in detail. In this

analysis, the cation and anion exchange membranes are assumed to have symmetrically identical selectivity. That is, the magnitude of the three phenomena are exactly the same in both CEM and AEM but of opposite polarity for co-ion transport.

a. *Co-ion Transport.* Due to the high concentration of fixed charges within the ion exchange membranes, the co-ions concentration within the charged membrane is much lower than counter-ions.[12, 13] This phenomenon is termed Donnan exclusion, and enables the membranes to preferentially select for counter-ions. Although the co-ion concentration in the membrane matrix is small, nonetheless they are not completely excluded and are, thus, still slightly permeable across the CEMs and AEMs. To quantify the relative leakage of co-ions, we introduce a dimensionless parameter, β:

$$\beta \equiv \frac{\Delta n_{s,co}}{\Delta n_{s,ct}} \tag{12}$$

where Δn_s denotes the moles of salt transported across the membrane and subscripts "co" and "ct" indicates co-ions and counter-ions, respectively. I.e., $0<\beta<1$; perfectly selective membranes than only allow counter-ions transport has β of zero, whereas β = 1 represents the migration of Na^+ and Cl^- ions in equal pairs (i.e., non-selective membrane). Hence, the total salt transport (counter- and co-ions) from the HC solution to the LC solution, is related to the salt permeating across the IEMs as counter-ions only, by the factor $1+\beta$.

Note that in an actual RED process, the ratio of counter ion to co-ion flux is not a fixed constant but, rather, depends on the actual current density. By using an external load of very high resistance, the current density is significantly lowered and relatively less counter ions are transported across the IEMs, thereby elevating the ratio in eq 12. In this study, the resistance of the external load is comparable to the internal resistance of the RED cell and, therefore, a constant β was used to simplify the analysis.

Assuming co-ions migrate across the membranes by Fickian diffusion, the co-ion flux, $J_{s,co}$, can be expressed as[16]

$$J_{s,co} = \frac{D_s}{\delta_m} \Delta c_s \tag{S3}$$

where D_s is the effective diffusion coefficient of co-ions in the ion exchange membranes, δ_m is membrane thickness, and Δc_s is the salt (or co-ion) molar concentration difference between the HC and LC solutions.

b. *Osmosis.* Ion exchange membranes are hydrated polymeric thin-films and, thus, are pervious to water.[14, 16] The salt concentration difference across the IEMs produces an osmotic gradient that drives the migration of water from the LC solution to the more salty HC solution. Again, we assume that the osmotic water flux across the membranes, $J_{w,os}$, is governed by Fickian diffusion:[16]

$$J_{w,os} = \frac{D_w}{\delta_m}\Delta c_w \approx -\frac{D_w}{\delta_m}\Delta c_s \tag{S4}$$

where D_w is the effective diffusion coefficient of water in the membranes and Δc_w is the molar concentration difference of water across the membranes. For the relatively dilute salt concentrations investigated in this study, the difference in water concentration can be approximated by the magnitude of the salt concentration difference, Δc_s. Dividing eq S4 by eq S3 yields:

$$\frac{D_w}{D_s} = -\frac{J_{w,os}}{J_{s,co}} \tag{S5}$$

As the water flux and co-ion flux are the rate of water and co-ions permeation per unit membrane area, respectively, the ratio of water to co-ion diffusivity in the membrane matrix, D^R, in eq S5 is also the mole ratio of water to co-ion transported across the membranes:

$$D^R \equiv \frac{D_w}{D_s} = -\frac{\Delta V_{os}}{\Delta n_{s,co}\overline{V}} \tag{14}$$

where ΔV_{os} is the volume of water transported by osmosis, $\overline{V}$ is the molar volume of water (i.e., $\Delta V_{os}/\overline{V}$ gives the moles of water), and $\Delta n_{s,co}$ denotes the moles of salt transported across the membrane as co-ions (as defined earlier). Note that the negative sign indicates water osmosis is in opposite direction to salt migration. A recent study indicates that the diffusion coefficient of salt in a swollen polymer is dependent on the

salt concentration of the surrounding solution.[17] For the ion exchange membranes considered here, we assume that the ratio D^R remains constant over the range of solution concentration examined in this study, to simplify the analysis.

c. *Electro-osmosis.* Charged ions migrating across a hydrated IEM exert an electrostatic field that drags along nearby polar water molecules.[14, 15] This phenomenon is termed electro-osmosis and induces a water flux in the direction of ion transport (i.e., against the osmotic gradient). As water migration due to electro-osmosis is proportional to the total ion flux[15, 16], we can introduce a dimensionless constant, h, to relate the transport of the two species:

$$h = \frac{\Delta V_{eo}}{\left(\Delta n_{s,ct} + \Delta n_{s,co}\right)\overline{V}} \tag{15}$$

where ΔV_{eo} is the volume of water transported by electro-osmosis (i.e., $\Delta V_{eo}/\overline{V}$ gives the moles of water) and $\Delta n_{s,ct}+\Delta n_{s,co}$ is the total moles of salt permeated.

The effect of co-ion transport, osmosis, and electro-osmosis in ion exchange membranes can be determined by experimental measurements and is describe in previous studies.[16, 18-21] Combining the effects of osmosis and electro-osmosis and using eq 12, the ratio of the total volume of water migrating across the ion exchange membranes, ΔV, to the salt permeating as counter-ions is

$$\frac{\Delta V}{\Delta n_{s,ct}} = \overline{V}\left[\beta D^R - h\left(1+\beta\right)\right] \tag{S6}$$

Alternatively, we define θ to be the mole ratio of water to salt (both counter- and co-ions) permeation across the membranes:

$$\theta \equiv \frac{\Delta V}{\left(\Delta n_{s,ct} + \Delta n_{s,co}\right)\overline{V}} = \frac{\beta}{1+\beta} D^R - h \tag{17}$$

Note that, henceforth, Δn_s denotes the moles of salt transported as counter-ions.

The concentration of the LC and HC solutions during RED with membrane selectivity imperfections are:

$$c_{\mathrm{LC}} = \frac{n_{\mathrm{s,LC}}^{0} + (1+\beta)\Delta n_{\mathrm{s}}}{V_{\mathrm{LC}}^{0} - (1+\beta)\theta\bar{V}\Delta n_{\mathrm{s}}} \tag{S7}$$

$$c_{\mathrm{HC}} = \frac{n_{\mathrm{s,HC}}^{0} - (1+\beta)\Delta n_{\mathrm{s}}}{V_{\mathrm{HC}}^{0} + (1+\beta)\theta\bar{V}\Delta n_{\mathrm{s}}} \tag{S8}$$

The fraction of salt in the initial HC solution that is transported as counter-ions can be determined by solving for $\Delta n_{\mathrm{s}}^{f}$ when $c_{\mathrm{LC}}^{f} = c_{\mathrm{HC}}^{f}$:

$$\frac{\Delta n_{\mathrm{s}}^{f}}{n_{\mathrm{s,HC}}^{0}} = \frac{\phi}{(1+\beta)\left(1+\theta\bar{V}c_{\mathrm{M}}^{f}\right)}\left(1-\frac{c_{\mathrm{LC}}^{0}}{c_{\mathrm{HC}}^{0}}\right) \tag{16}$$

Note that setting β and θ to zero in eq 16 recovers eq 3 of the main manuscript, the fraction of salt eventually transported for perfectly selective membranes.

For the 1:1 NaCl electrolyte solutions (i.e., $z_{+} = z_{-} = z = 1$) considered in this analysis and assuming that the CEM and AEM have identical permselectivity (i.e., $\alpha_{\mathrm{CEM}} = \alpha_{\mathrm{AEM}} = \alpha$), the electromotive force of a one-cell RED, ξ_{emf} (eq 1), with imperfect selectivity is

$$\xi_{\mathrm{emf}} = \frac{\alpha\nu R_{\mathrm{g}}T}{zF}\ln\frac{c_{\mathrm{HC}}}{c_{\mathrm{LC}}} \tag{S9}$$

where ν is the number of ions each salt molecule dissociates into (ν is 2 for NaCl employed in this analysis), R_{g} is the gas constant, T is the absolute temperature, z is the ion valence (i.e., $z = 1$ for Na^{+} and Cl^{-}), and F is the Faraday constant. Similar to the earlier discussion, the activity coefficient, γ, is simplified to be unity without significantly affecting the accuracy of the analysis. A previous study applied the first principles of Donnan potential and electric potential across an ion exchange membrane in the Teorell, Meyer, Sievers model and derived the membrane permselectivity:[22]

$$\alpha = t_{\mathrm{ct}} - t_{\mathrm{co}} \tag{S10}$$

The transport number, t, is defined as the fraction of total ions that is transported across the IEM as counter- or co-ions (denoted by subscripts ct and co, respectively). Based on the definition of the terms, $t_{\mathrm{ct}} = 1/(1+\beta)$ and $t_{\mathrm{co}} = \beta/(1+\beta)$.[23] Therefore, the membrane permselectivity can also be expressed as

$$\alpha = \frac{1-\beta}{1+\beta} \tag{13}$$

Substituting eqs S7 and S8 into eq S9 gives the electromotive force, ξ_{emf}, across the one-cell RED (depicted in Figure 1B of the main manuscript) during the process with imperfections in the selectivity of the ion exchange membranes:

$$\xi_{\text{emf}} = \frac{\alpha \nu R_{\text{g}} T}{zF}\left(\ln \frac{n_{\text{s,HC}}^{0} - (1+\beta)\Delta n_{\text{s}}}{V_{\text{HC}}^{0} + (1+\beta)\theta\overline{V}\Delta n_{\text{s}}} - \ln \frac{n_{\text{s,LC}}^{0} + (1+\beta)\Delta n_{\text{s}}}{V_{\text{LC}}^{0} - (1+\beta)\theta\overline{V}\Delta n_{\text{s}}} \right) \tag{S11}$$

Imperfect Membrane Selectivity Gives Rise to Uncontrolled Mixing in RED. Apart from diminishing the effective driving force for ion flux and lowering Δn_{s}^{f}, the undesirable migration of co-ions also negates an equal charge of counter-ions permeating across the CEM and AEM in Figure 1B. Therefore, to obtain the useful work extractable in RED with imperfectly selective membranes, a factor of $(1-\beta)$ is incorporated into the variable of integration, Δn_{s}, in the integration of the external potential difference. I.e., if the membranes are completely unselective for counter-ions ($\beta = 1$), the net ion flux is zero and no work is produced as the ions migrate across each IEM as cation-anion pairs. By employing an external load of infinitely large resistance, the potential difference across the load, ξ_{L}, approaches ξ_{emf} (eq S11). Under this scenario, integrating ξ_{L} (or, equivalently, ξ_{emf}) across the charges transferred yields the maximum work per unit volume of the LC solution with imperfectly selective membranes:

$$W_{\text{Imp},V_{\text{LC}}^{0}} = zF\int_{0}^{\Delta n_{\text{s}}^{f}} \xi_{\text{emf}}\, d(1-\beta)\Delta n_{s} = \alpha^{2}\left\{ \Delta G_{\text{mix},V_{\text{LC}}^{0}} - \frac{\nu R_{g} T}{\theta\overline{V}}\left[\begin{array}{l} \dfrac{1-\phi}{\phi}\left(1+\theta\overline{V}c_{\text{HC}}^{0}\right)\ln\left(1+\theta\overline{V}c_{\text{HC}}^{0}\right) \\ +\left(1+\theta\overline{V}c_{\text{LC}}^{0}\right)\ln\left(1+\theta\overline{V}c_{\text{LC}}^{0}\right) \\ -\dfrac{1}{\phi}\left(1+\theta\overline{V}c_{\text{M}}^{f}\right)\ln\left(1+\theta\overline{V}c_{\text{M}}^{f}\right) \end{array} \right] \right\} \tag{18}$$

which is eq 18 of the main manuscript.

REFERENCES

1. Bockris, J. O. M.; Reddy, A. K. N.; Gamboa-Aldeco, M. E., *Modern electrochemistry*. 2nd ed.; Plenum Press: New York, **1998**.

2. Yip, N. Y.; Elimelech, M., Thermodynamic and Energy Efficiency Analysis of Power Generation from Natural Salinity Gradients by Pressure Retarded Osmosis. *Environ Sci Technol* **2012,** *46*, (9), 5230-5239.

3. Weinstein, J. N.; Leitz, F. B., Electric-Power from Difference in Salinity - Dialytic Battery. *Science* **1976,** *191*, (4227), 557-559.

4. Dlugolecki, P.; Gambier, A.; Nijmeijer, K.; Wessling, M., Practical Potential of Reverse Electrodialysis As Process for Sustainable Energy Generation. *Environ Sci Technol* **2009,** *43*, (17), 6888-6894.

5. Post, J. W.; Hamelers, H. V. M.; Buisman, C. J. N., Energy recovery from controlled mixing salt and fresh water with a reverse electrodialysis system. *Environ Sci Technol* **2008,** *42*, (15), 5785-5790.

6. Długołęcki, P.; Anet, B.; Metz, S. J.; Nijmeijer, K.; Wessling, M., Transport limitations in ion exchange membranes at low salt concentrations. *J Membrane Sci* **2010,** *346*, (1), 163-171.

7. Robinson, R. A.; Stokes, R. H., *Electrolyte solutions; the measurement and interpretation of conductance, chemical potential, and diffusion in solutions of simple electrolytes*. 2d ed.; Butterworths: London,, **1959**; p xv, 571 p.

8. Dlugolecki, P.; Nymeijer, K.; Metz, S.; Wessling, M., Current status of ion exchange membranes for power generation from salinity gradients. *J Membrane Sci* **2008,** *319*, (1-2), 214-222.

9. Güler, E.; Elizen, R.; Vermaas, D. A.; Saakes, M.; Nijmeijer, K., Performance-determining membrane properties in reverse electrodialysis. *J Membrane Sci* **2013,** *446*, 266-276.

10. Veerman, J.; Saakes, M.; Metz, S. J.; Harmsen, G. J., Reverse electrodialysis: A validated process model for design and optimization. *Chem Eng J* **2011,** *166*, (1), 256-268.

11. Vermaas, D. A.; Saakes, M.; Nijmeijer, K., Doubled Power Density from Salinity Gradients at Reduced Intermembrane Distance. *Environ Sci Technol* **2011,** *45*, (16), 7089-7095.

12. Baker, R. W., *Membrane technology and applications*. 3rd ed.; John Wiley & Sons: Chichester, West Sussex ; Hoboken, **2012**; p xiv, 575 p.

13. Mulder, M., *Basic principles of membrane technology*. 2nd ed.; Kluwer Academic: Dordrecht ; Boston, **1996**; p 564 p.

14. Belfort, G., *Synthetic membrane processes : fundamentals and water applications*. Academic Press: Orlando, Fla., **1984**; p xiii, 552 p.

15. Spiegler, K. S., Transport processes in ionic membranes. *Transactions of the Faraday Society* **1958,** *54*, 1408-1428.

16. Veerman, J.; de Jong, R. M.; Saakes, M.; Metz, S. J.; Harmsen, G. J., Reverse electrodialysis: Comparison of six commercial membrane pairs on the thermodynamic efficiency and power density. *J Membrane Sci* **2009,** *343*, (1-2), 7-15.

17. Geise, G. M.; Freeman, B. D.; Paul, D. R., Sodium chloride diffusion in sulfonated polymers for membrane applications. *J Membrane Sci* **2013,** *427*, 186-196.

18. Berezina, N.; Gnusin, N.; Dyomina, O.; Timofeyev, S., Water electrotransport in membrane systems. Experiment and model description. *J Membrane Sci* **1994,** *86*, (3), 207-229.

19. Berezina, N. P.; Kononenko, N. A.; Dyomina, O. A.; Gnusin, N. P., Characterization of ion-exchange membrane materials: Properties vs structure. *Advances in Colloid and Interface Science* **2008,** *139*, (1–2), 3-28.

20. Barragan, V. M.; Rueda, C.; Ruizbauza, C., On the Fixed Charge Concentration and the Water Electroosmotic Transport in a Cellulose-Acetate Membrane. *J Colloid Interf Sci* **1995,** *172*, (2), 361-367.

21. Barragan, V. M.; Ruiz-Bauza, C., Membrane potentials and electrolyte permeation in a cation-exchange membrane. *J Membrane Sci* **1999,** *154*, (2), 261-272.

22. Lakshminarayanaiah, N., Transport Phenomena in Artificial Membranes. *Chemical Reviews* **1965,** *65*, (5), 491-565.

23. Strathmann, H., *Ion-exchange membrane separation processes*. 1st ed.; Elsevier: Amsterdam ; Boston, **2004**; p xi, 348 p.

NOMENCLATURE

Acronyms

AEM	anion exchange membrane
ASR	area specific resistance
CEM	cation exchange membrane
emf	electromotive force
HC	high concentration
IEM	ion exchange membrane
LC	low concentration
PD	power density
RED	reverse electrodialysis
TDS	total dissolved solids

Symbols

A	effective cell area
c	molar salt concentration
Δc_s	salt (or co-ion) molar concentration difference across membrane
Δc_w	water molar concentration difference across membrane
d	intermembrane distance
D_s	effective diffusion coefficient of salt (as co-ion) in membrane
D_w	effective diffusion coefficient of water in membrane
D^R	ratio of water diffusivity to salt (as co-ion) diffusivity in membrane matrix
F	Faraday constant

ΔG_{mix}	Gibbs free energy of mixing
$\Delta G_{\text{mix},V_{\text{LC}}^0}$	specific Gibbs free energy of mixing (energy per unit volume of initial low concentration solution)
h	mole ratio of water permeated by electro-osmosis to salt (both counter- and co-ions) permeated
i	current density (or molar ion flux $\times z \times F$)
I	electric (or ionic) current
J_{s}	salt flux
J_{w}	water flux
N	number of membrane pairs (or repeating RED cells)
n_{s}	moles of salt
Δn_{s}	moles of salt permeated
PD_{avg}	overall membrane power density
P_{L}	useful power generated by external load
Δq	coulombs of ion permeated
r	internal resistance
R_{L}	resistance of external load
R_{g}	gas constant
t	transport number
T	absolute temperature
V	volume of solution
ΔV	volume of water permeated
$\bar{V}$	molar volume of pure water
W	extractable work in irreversible thermodynamic RED

W_{ideal}	ideal work
$W_{\text{ideal},V_{\text{LC}}^0}$	specific ideal work (energy per unit volume of initial low concentration solution)
$W_{\text{Imp},V_{\text{LC}}^0}$	specific maximum energy extractable with imperfectly selective ion exchange membranes
x	ion mole fraction
z	ion valency

Greek Symbols

α	ion exchange membrane permselectivity
β	mole ratio of co-ions to counter-ions transported across the membranes
γ	ion activity coefficient
δ_{m}	membrane thickness
η	energy conversion efficiency
θ	mole ratio of water to salt (both counter- and co-ions) permeation
κ	solution electrical conductivity
Λ	molar conductivity
ν	number of ions each salt molecule dissociates into
ξ	potential difference
ϕ	ratio of total moles (or volume) of the low concentration solution to total moles (or volume) of the system

Superscripts

0	initial
f	final
*	optimum parameter where overall power density in RED with constant resistance external load is maximized

Subscripts

–	anion
+	cation
½emf	electromotive force of RED half-cell
AEM	anion exchange membrane
CEM	cation exchange membrane
cell	one repeating RED cell
co	co-ions
ct	counter-ions
emf	electromotive force
el	end electrodes and redox couple
eo	electro-osmosis
HC	high concentration solution
L	external load
LC	low concentration solution
M	resultant mixture
os	osmosis
stack	reverse electrodialysis stack

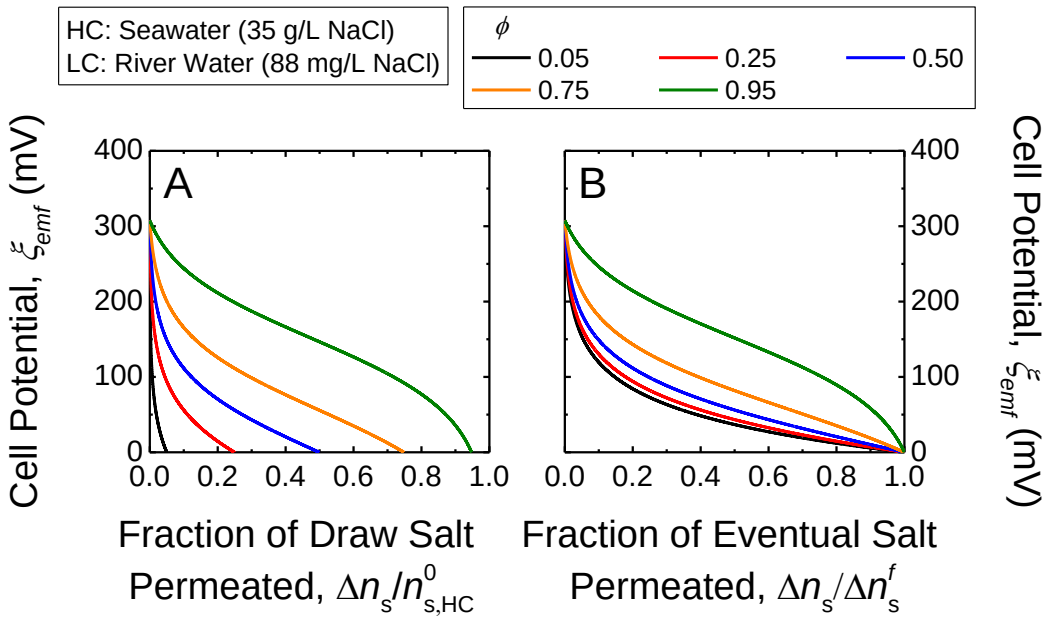

Figure S1. Electric potential (or electromotive force), ξ_{emf}, across a one-cell RED (as depicted in Figure 1B of the main manuscript), as a function of A) the fraction of salt in the HC solution that has permeated across the ion exchange membranes, $\Delta n_s / n^0_{s,HC}$, and B) the fraction of salt that eventually migrates across the membranes, $\Delta n_s / \Delta n^f_s$. The plots for a range of ϕ (volumetric ratio of the LC solution to both the HC and LC solutions) are presented. The HC solution is seawater (600 mM or 35 g/L NaCl), the LC solution is river water (1.5 mM or 88 mg/L NaCl), and the IEMs are assumed to be perfectly selective for counter ions (i.e., α = 1). Based on the Nernst equation with temperature of 298 K, the initial potential across the RED cell is 308 mV (eq 1). The horizontal axis intercepts of plot A) signify the fraction of salt in the initial HC solution that will ultimately permeate across the membrane ($\Delta n^f_s / n^0_{s,HC}$, eq 3). For low volumetric fractions of initial LC solution volume, e.g., ϕ = 0.05, the salt concentration of the LC solution rises rapidly as ions permeate across the ion exchange membranes. Thus, ξ_{emf} declines steeply and only a relatively small fraction of HC salt is transported across the membranes. Conversely, for large ϕ, the permeated salt is diluted by the large LC solution volume and, hence, a greater fraction of salt is transported from the HC solution. The specific ideal work (extractable energy per unit volume of the initial LC solution) for a reversible thermodynamic RED process can be calculated from the area under each curve (eq 5).

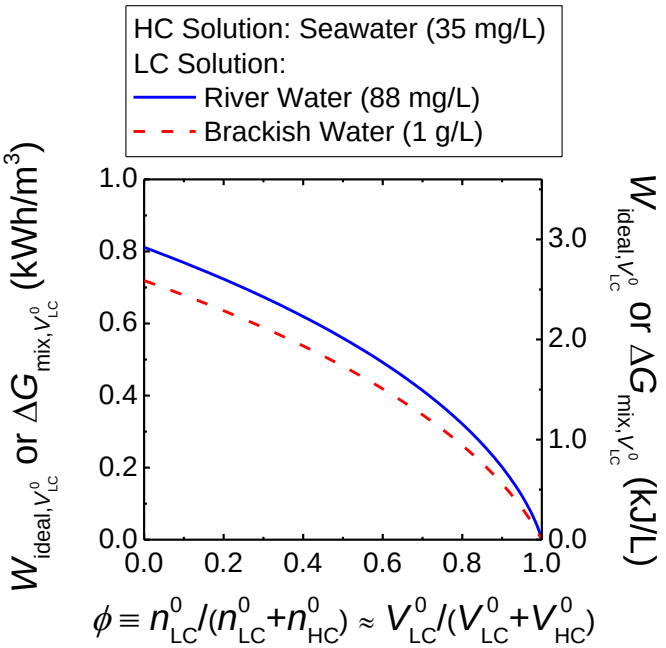

Figure S2. Specific ideal work, W_{ideal,V_{LC}^0}, as a function of the mole fraction of the fresh river or brackish water (LC solution) to both the fresh water and seawater (LC and HC solution), ϕ. The ideal work extractable is expressed as the energy per unit volume of the LC solution and is equivalent to the Gibbs free energy of mixing, $\Delta G_{mix,V_{LC}^0}$, in reversible thermodynamic RED (eq 6). The calculations were carried out for a temperature of 298 K, and the concentration of seawater HC solution was assumed to be 600 mM (35 g/L) NaCl, while the concentrations of river water and brackish water LC solution were taken to be 1.5 and 17 mM (88 mg/L and 1 g/L) NaCl, respectively. For the dilute concentrations considered here, the mole fraction can be approximated to be the volumetric fraction of the LC solution.

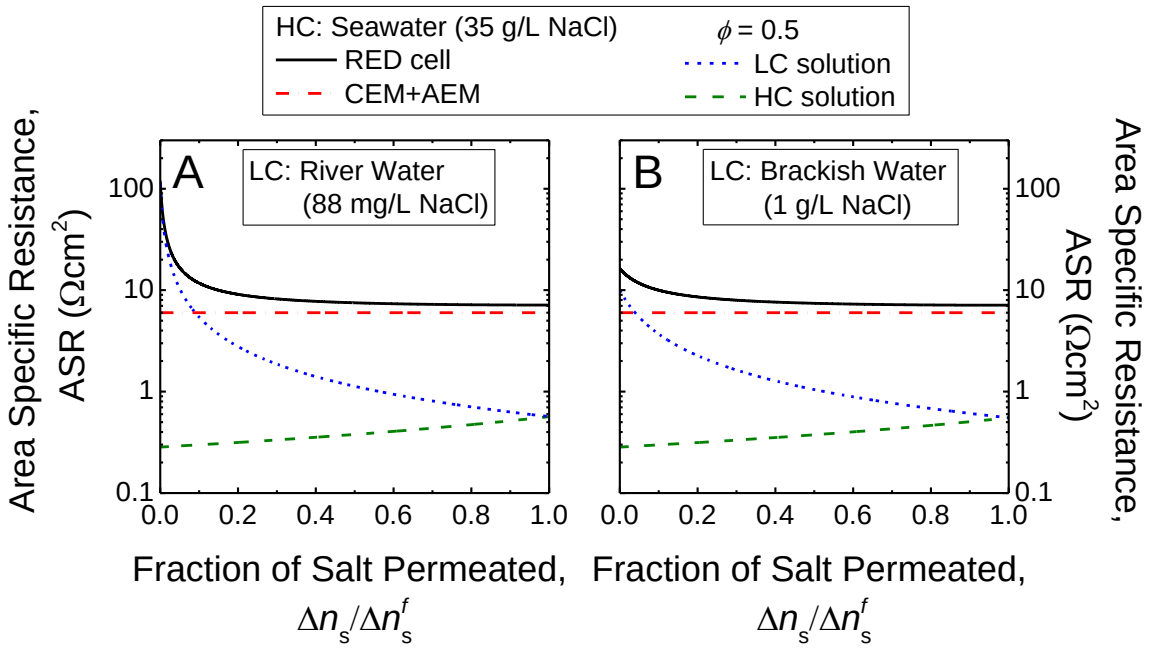

Figure S3. Representative plot of the area specific resistance, ASR, of the RED cell and its components (i.e., HC solution, LC solution, and CEM and AEM), as a function of the fraction of salt that has permeated across the ion exchange membranes, $\Delta n_s / \Delta n_s^f$. Seawater (600 mM or 35 g/L NaCl) is employed as the HC solution, while the LC solution is (A) 1.5 mM or 88 mg/L NaCl river water or (B) 17 mM or 1 g/L NaCl brackish water. The solid black lines denote the total ASR of the one-cell RED, while the contribution from each stack element: CEM and AEM, LC solution chamber, and HC solution chamber are indicated by dash-dotted red lines, dotted blue lines, and dashed green lines, respectively. The IEMs are assumed to be perfectly selective (i.e., completely excludes co-ions and no water permeation). The ASR of the ion exchange membranes (i.e., CEM and AEM) are both 3.0 Ωcm^2. The solution conductivity, $\kappa = \Lambda c$, where Λ (= 0.08798 mS cm^{-1}mM^{-1}) is the molar conductivity of sodium chloride solutions and c is the salt concentration. The ASR of the solutions are calculated by multiplying the intermembrane distance, d = 150 μm, by the reciprocal of κ. Note that the vertical axes are on a logarithmic scale. The volumetric fraction of the LC solution, ϕ, is 0.5, and temperature T = 298 K.

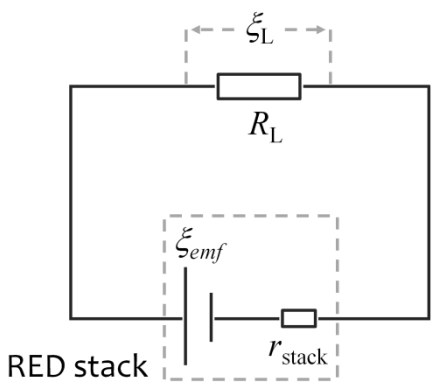

Figure S4. Schematic of an RED circuit, comprising the RED stack of potential ξ_{emf} and internal resistance r_{stack}, and external load of resistance R_L. The potential difference across the external load is $\xi_L = \xi_{emf} R_L/(R_L+r_{stack})$.

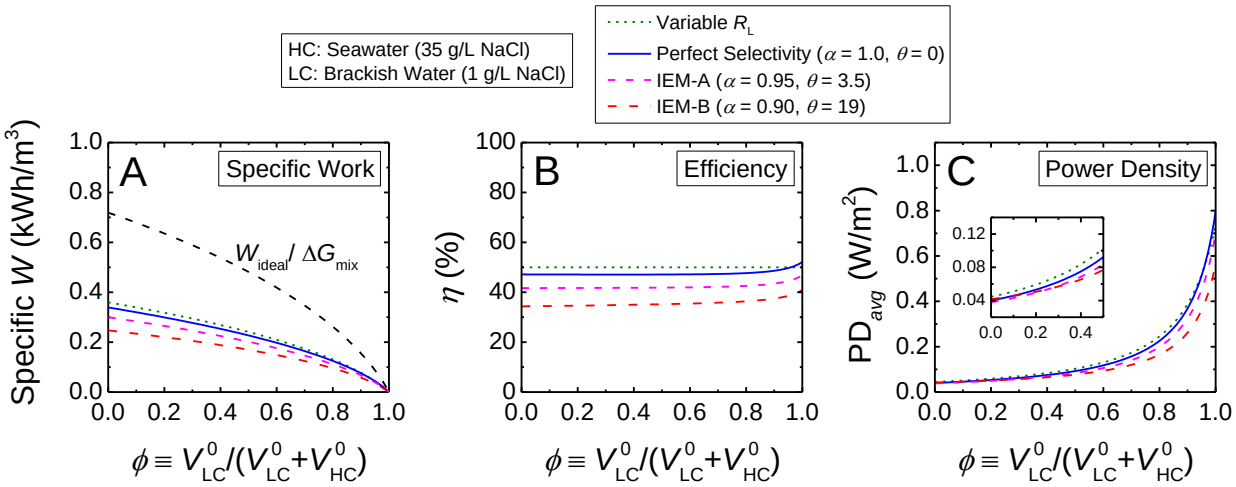

Figure S5. (A) Extractable work per unit volume of the LC solution, specific W^*, (B) energy conversion efficiency, η, and (C) overall membrane power density, PD_{avg}, of RED energy production as a function of the volumetric fraction of LC solution to both LC and HC solutions, ϕ. The dashed black line in (A) indicates the ideal work extractable in a reversible thermodynamic RED process, $W_{\text{ideal},V_{LC}^0}$, which is equivalent to the Gibbs free energy of mixing, $\Delta G_{\text{mix},V_{LC}^0}$. The solid blue lines, dashed magenta lines, and dash-dotted red lines indicate a perfectly selective membrane (i.e., α = 1 and θ = 0), IEM-A with moderately imperfect selectivity (α = 0.95 and θ = 3.5), and IEM-B with more severe selectivity imperfections (α = 0.90 and θ = 19), respectively. The dotted green lines indicate the theoretical performance achieved with perfectly selective membranes when the resistance of the external load is varied such that it exactly matches the RED stack resistance throughout the process (i.e., $R_L = r_{cell}$). In this hypothetical case, η is always 50% and PD is maximized. Magnified plot of (C) for $0<\phi<0.5$ is shown in the inset. Seawater (600 mM or 35 g/L NaCl) is employed as the HC solution, brackish water (17 mM or 1 g/L NaCl) is used as the LC solution, and temperature T = 298 K. The area specific resistance, ASR, of the membranes is 3.0 Ωm^2 and the intermembrane distance, d, is 150 μm.

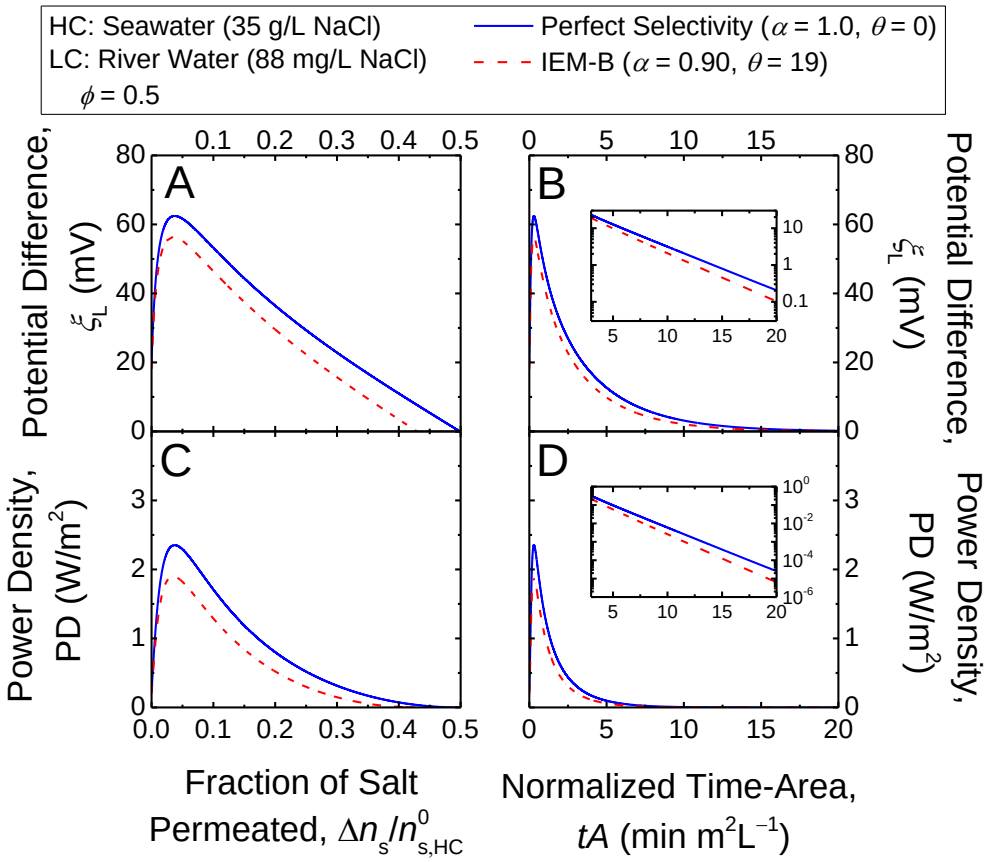

Figure S6. Top row: representative plots of potential difference across the constant resistance external load, ξ_L, as a function of (A) the fraction of salt that has permeated across the ion exchange membranes, $\Delta n_s / n^0_{s,HC}$, and (B) normalized time-area, tA. Normalized time-area is defined as the time per unit total volume of the HC and LC solutions, multiplied by the effective cross-sectional area of the RED cell depicted in Figure 1B of the main manuscript. I.e., using large solution volumes or a smaller effective area would lengthen the process duration. Bottom row: Representative plots of power density, PD, as a function of (C) $\Delta n_s / n^0_{s,HC}$ and (D) tA. Insets of (B) and (D) shows magnified plots from $3<tA<20$ min m^{2}L^{-1} with logarithmic scale for the vertical axes. The solid blue lines and dash-dotted red lines indicate perfectly selective membranes (i.e., α = 1 and θ = 0) and IEM-B with selectivity imperfections (α = 0.90 and θ = 19). The area specific resistance of the CEM and AEM are both 3.0 Ωm^2 and the intermembrane distance is 150 μm. Seawater (600 mM or 35 g/L NaCl) is employed as the HC solution, river water (1.5 mM or 88 mg/L NaCl) is used as the LC solution, ϕ = 0.5, and temperature T = 298 K.

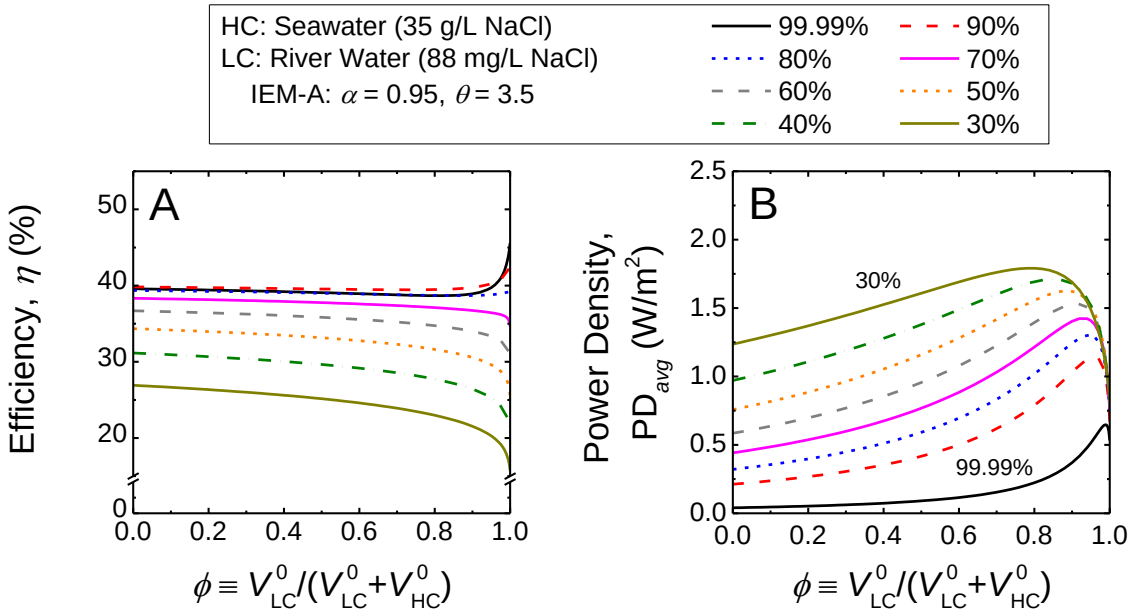

Figure S7. (A) Energy conversion efficiency, η, and (B) overall membrane power density, PD_{avg}, as a function of the volumetric fraction of LC solution to both LC and HC solutions, ϕ. The plots show performance of RED energy production when the process is terminated prematurely, thereby utilizing only the earlier transported charges for power generation and discarding the remainder. A range of charge utilization percentages (99.99, 90, 80, 70, 60, 50, 40, and 30%) are presented. The ion exchange membranes have moderately imperfect selectivity (i.e., IEM-A with $\alpha = 0.95$ and $\theta = 3.5$). Seawater (600 mM or 35 g/L NaCl) is employed as the HC solution, river water (1.5 mM or 88 mg/L NaCl) is used as the LC solution, and temperature T = 298 K. For this analysis, the intermembrane distance, d, is 150 μm and the ion exchange membrane area specific resistance, ASR, is 3.0 Ωcm^2.

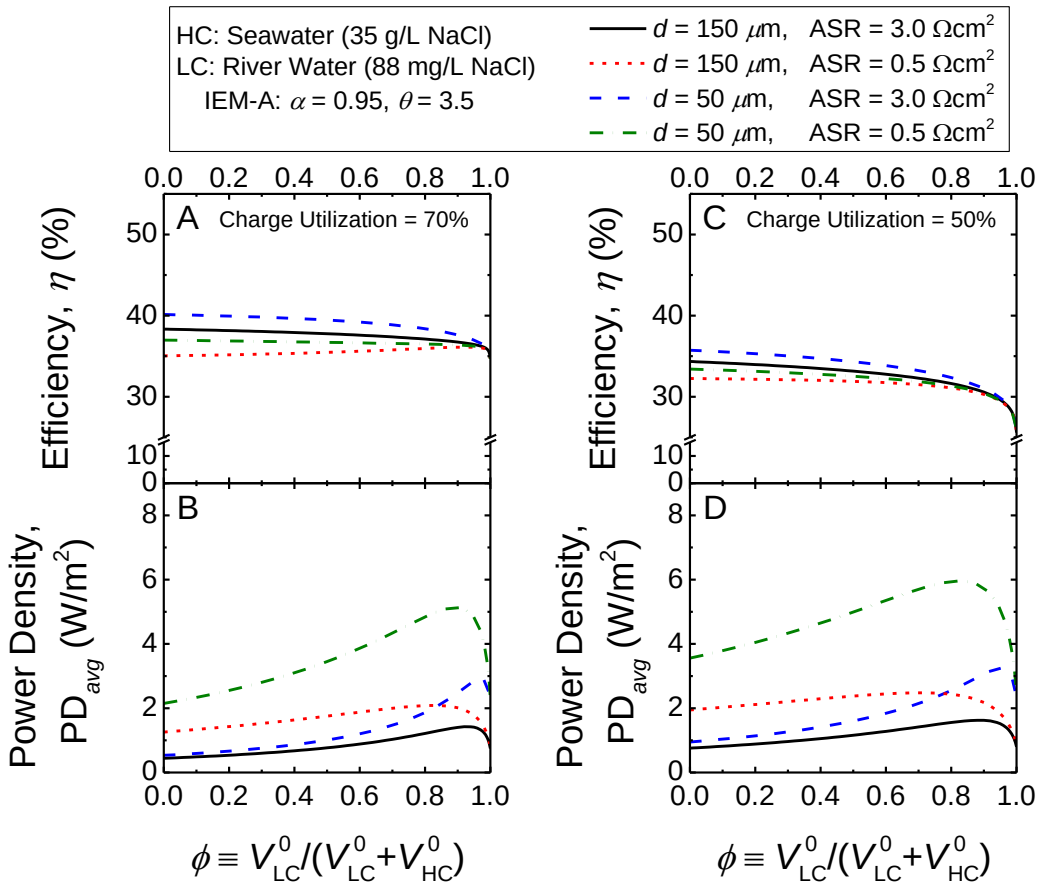

Figure S8. (A) and (C) Energy efficiency, η, and (B) and (D) overall membrane power density of RED energy production, PD_{avg}, as a function of the volumetric fraction of LC solution to both LC and HC solutions, ϕ. The lines denote RED cells with different ion exchange membrane area specific resistances (ASR = 0.5 or 3.0 Ωcm^2) and intermembrane distances (d = 50 or 150 μm). For all four scenarios, the CEM and AEM have moderately imperfect selectivity (i.e., IEM-A with α = 0.95 and θ = 3.5). For (A) and (B) on the left, 70% of the charges were utilized for power generation, while (C) and (D) on the right utilized 50% of the charges. Seawater (600 mM or 35 g/L NaCl) is employed as the HC solution, river water (1.5 mM or 88 mg/L NaCl) is used as the LC solution, and temperature T = 298 K.